Int J Adv Manuf Technol (2009) 45:679–689
DOI 10.1007/s00170-009-2007-x

ORIGINAL ARTICLE

Prediction of optimal stability states in inward-turning operation using neurogenetic algorithms

K. Rama Kotaiah · J. Srinivas · M. Sekar

Received: 4 November 2008 / Accepted: 6 March 2009 / Published online: 21 March 2009

Abstract This paper proposes a neurogenetic-based optimization scheme for predicting localized stable cutting parameters in inward turning operation. A set of cutting experiments are performed in inward orthogonal turning operation. The cutting forces, surface roughness, and critical chatter locations are predicted as a function of operating variables including tool overhang length. Radial basis function neural network is employed to develop the generalization models. Optimum cutting parameters are predicted from the model using binary-coded genetic algorithms. Results are illustrated with the data corresponding to four work materials, i.e., EN8 steel, EN24 steel, mild steel, and aluminum operated over a high speed steel tool.

Keywords Critical chatter length · Tool overhang · Neural networks · Optimum parameters · Orthogonal turning

Nomenclature

v	Cutting speed (m/min)
f	Feed rate (mm/rev)
d	Depth of cut (mm) = DOC
l	Tool overhang length (mm)
HSS	High speed steel
CCL (C_c)	Critical chatter length(mm)
F_x, F_y, F_z	Cutting forces in x, y, and z directions in Newton
V_o	Optimum cutting speed (m/min)
f_o	Optimum feed rate(mm/rev)
d_o	Optimum depth of cut (mm)
f_w	Flank wear (mm)
R_a	Surface roughness (μm)

K. Rama Kotaiah (✉)
Department of Industrial and Production Engineering,
K.L. College of Engineering,
Vaddeswaram,
Guntur 522502, Andhra Pradesh, India
e-mail: krk_ipe@yahoo.co.in

J. Srinivas · M. Sekar
School of Mechanical Engineering,
Kyungpook National University,
Daegu, South Korea

1 Introduction

The most detrimental phenomenon to productivity is unstable cutting. This reduces tool life and surface quality of workpiece. Many theoretical investigations are available in literature for prediction of stable and unstable cutting states in orthogonal cutting. In most of the cases, the stability lobe diagram is generated from an analytical linear model, by varying one operating parameter at a time. In orthogonal turning, it is well known that the cutting forces depend on the operating variables such as feed, depth of cut, and speed. These variables are often used to control the forces or machining stability by establishing appropriate regression relations. Recently, it is found that other parameters such as tool geometry [1], tool wear [2], variations in shear angle [3], and compliance of workpiece [4–6] have great influence on cutting dynamics. To distinguish stability states of cutting, the output features such as surface roughness [7, 8] and type of chips [9] can be employed effectively in addition to cutting force data and stability states. In practice, there are several other operating parameters like tool overhanging length and type of material that may also have influence on the critical operating conditions. For example, variation of tool overhang length changes the stiffness of tool holder, which in turn alters the tool wear and life during unstable conditions. Likewise, the effects of cutting fluids on the surface roughness and tool wear have been predicted [10]. In

another work [11] studied the overall influence of amount of lubrication along with cutting speed and feed rates on the surface roughness and specific cutting forces which in turn directly affect the stability of the process. In this paper, the cross-section dimension of the workpiece, tool stiffness, and damping ratios effect on dynamics of the system is neglected because the effect of all the parameters is explained in [12].

In this paper, the effects of cutting parameters in orthogonal turning operation including tool overhang length on the critical chatter lengths over the workpiece and the static cutting forces on the tool are studied. A series of cutting experiments are carried out using four different work materials, i.e., EN24 steel, EN8 steel, mild steel, and aluminum at various operating speeds, feeds, and depths of cut. In all cases, dynamic cutting forces, surface roughness, and critical chatter lengths are measured. Relations between the input and output parameters are established using radial-basis function (RBF) neural network model and it is further employed to arrive at the optimized machining data within the operating constraints using genetic algorithms (GA). Brief description of proposed neural network model and optimization scheme through GA is presented in Section 3 and the numerical results and discussions are given in Section 4. The following section briefly describes the experimental analysis to obtain the parametric data.

2 Experimental analysis

In present analysis, a series of cutting experiments are carried out on a workshop center lathe in order to find the critical stability state in inward turning. Figure 1 show the experimental setup employed in the present work. Cutting is performed from the collar end of the workpiece.

The cutting operation is carried out for short cutting length only and operation is inward turning operation. The cutting speed (v), feed rate (f), depth of cut (d), and tool overhang length (l) are progressively varied to obtain the cutting forces (feed force, radial force, and tangential force), surface roughness, and critical chatter lengths (CCL) on the workpiece. The measured critical chatter lengths are taken from the free end of the workpiece and tail stock support is taken in every experiment. Ranges of each cutting parameter and their associated levels are depicted in Table 1. In all the cases, 50-mm-diameter workpieces are employed and tool material is HSS S-200. An attached tool post strain gauge dynamometer platform is used to measure the cutting forces in three directions. The required feed rate is chosen from the lathe preset arrangement. In this study, the influence of tool overhanging length on the cutting forces developed, surface roughness obtained, and critical chatter length during turning operation was evaluated. In order to examine the influence of tool overhanging length, turning tests are carried out on EN24 steel, EN8 steel, mild steel, and aluminum workpieces using four different tool overhanging lengths. The turning tests at each tool overhanging length were conducted at three different cutting speeds while depth of cut, feed rate, and tool angles were constant. Here, experiments are conducted at four different overhanging lengths and three different cutting speeds of 7, 14, and 22 m/min. Dynamometer is calibrated before applying loads on lathe. Calibration is done individually for horizontal and vertical forces with reference to proving ring and microvolt indicated on bridge balance unit is recorded with respect to definite known loading. Graph was plotted load verses microvolts for calibration of horizontal and vertical forces separately after multiplying with multiplication factor, i.e., 1 kg equal to 23.4 and 20.3 μV, respectively.

Fig. 1 Experimental setup

3 Proposed neurogenetic approach

Relationship between several operating variables and the output parameters is first obtained from the neural network model. For the last one decade, several works have been reported on the use of neural networks in modeling of turning process. Few recent applications of neural networks in turning operation include extraction of surface roughness information [13–16] and prediction of workpiece motions from cutting tool vibration signals [17]. There are many types of neural networks in common use. Main advantage of using neural networks is that the entire experimental data could be consolidated into few cutting parameters known as weights and centers. Figure 2 shows the schematic diagram of the proposed approach of obtaining the critical operating variables. Thus, function approximation module is used to obtain the relationship between the input and output data. After establishing the neural network model, it is employed to minimize the cutting forces under a range of input variables.

Table 1 Operating parameters and their levels used in the experiments

Workpiece material	Cutting speed v (m/min)	Feed rate f (mm/rev)	Depth of cut d (mm)	Tool overhang length l (mm)
EN24 steel	7, 14, and 22	0.1	0.1–0.7 with 0.1 interval	54, 57, 59, and 61
EN8 Steel	7, 14, and 22	0.1	0.1–0.7 with 0.1 interval	53, 57, 60, and 63
Mild Steel	7, 14, and 22	0.1, 0.138, 0.175, 0.2, 0.275, 0.35, and 0.5	0.1	54, 57, 59, and 61
Aluminum	7, 14, and 22	0.1, 0.138, 0.175, 0.2, 0.275, 0.35, and 0.5	0.1	53, 56, 58, and 62

3.1 RBF neural network

Of the available architectures, RBF neural network has principal advantages such as single hidden layer, training requiring at only output layer, and comparatively rapid convergence. RBF model has three layers: an input layer, a hidden layer of radial basis neurons, and an output layer of linear neurons [18]. The hidden layer consist of an array of computing units called hidden nodes. Each hidden node j contains a center vector C_j that is a parameter vector of the same dimension as the input data vector X and calculates the Euclidean distance between the center and the network input vector X defined by: $\|X - C_j\|$. The results are then passed through a nonlinear activation function (known as radial basis function) $\varphi_{\mathbf{j}}$, to produce the output from the hidden nodes. A popular choice of the activation function is the Gaussian basis function:

$$\varphi_j(t) = \exp\left[-\frac{\|X - C_j\|^2}{2\sigma_j^2}\right] j = 1, 2, 3, \ldots\ldots, M \tag{1}$$

where σ_j is a positive scalar that is called the width and M is the number of hidden units. It is often assumed that the number of hidden units is significantly less than the number of the data points. The constant width parameter of hidden unit controls the smoothness property of the activation function. When the width is small, the corresponding area of the representation space becomes small. Hence, a high number of centers will be required during the process of training. This results in overparameterization. On the contrary, the area of the representation space may be too extensive when the width σ is large. For both cases, the generalization capabilities of the network will be poor. Often σ_j is selected from the relation: $\sigma_j = \frac{d_{\max}}{\sqrt{2M}}$, where $d_{\max}$ is the maximum distance between the centers of hidden units. The center vector C_j is obtained from the K-means clustering algorithm in which all the input sets are arranged into clusters whose centers are initially chosen randomly from all the input sets. The output layer consists of p neurons and it is fully connected to the middle layer. Each linear output neurons forms the weighted sum of these radial basis functions. In other words, the network output:

$$\widehat{y_i} = \sum_{j=1}^{M} w_{ji}\varphi_j,\ i = 1, 2, 3, \ldots\ldots\ldots p \tag{2}$$

where φ_j is the response of the jth hidden unit resulting from all input data and w_{ji} is the connecting weight between the jth hidden unit and the ith output unit.

In matrix notation, Eq. 2 can be written as

$$\widehat{Y} = W\phi \tag{3}$$

where

$$W = \begin{bmatrix} w_{11} & w_{21} & \ldots\ldots & w_{M1} \\ w_{12} & w_{22} & \ldots\ldots & w_{M2} \\ \ldots\ldots & \ldots\ldots & \ldots\ldots & \ldots\ldots \\ w_{1p} & w_{2p} & \ldots\ldots & w_{Mp} \end{bmatrix} \tag{4}$$

and

$$\phi = [\varphi_1 \varphi_2 \ldots\ldots\ldots\ldots\ldots \varphi_M]^T. \tag{5}$$

By the end of passing all the input sets (known as epoch or cycle), a mean square error (MSE) is computed according to:

$$\mathrm{MSE} = \frac{1}{2\mathrm{PAT} \times p} \sum_{k=1}^{\mathrm{PAT}} \sum_{i=1}^{p} (y_i - \widehat{y_i})^2 \tag{6}$$

where PAT refers to the total number of patterns in each cycle and is the target value at the ith output layer. Weights

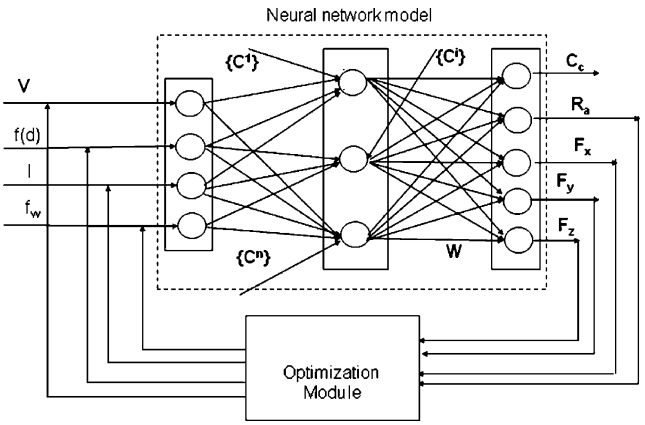

Fig. 2 Proposed neurogenetic approach

are updated using recursive least square or gradient descent algorithm according to

$$w_{ji}^{\text{new}} = w_{ji}^{\text{old}} + \alpha\varphi_j\left(y_i - \hat{y}_i\right) \tag{7}$$

where it is the learning parameter whose value is chosen between 0 and 1. After the learning phase, the network can be used to obtain the output for any unknown input pattern.

3.2 Genetic algorithms

GA also known as "evolution strategies" are optimization algorithms imitating principles of biological evolution. GA is a probabilistic search process based on natural genetic system; it is highly parallel and efficient optimization strategy and believed to be robust. GA is capable of solving wide range of complex optimization problems using three genetic operations: selection/reproduction, crossover, and mutation. The only "fittest" individuals of every generation survive to obtain the next generation. GA considers several points in the search space simultaneously and the chance of convergence to a local optimum is reduced. GA does not need the knowledge of the gradient of the fitness functions, which is very suitable for the optimization problems where an analytical expression for the fitness function is unknown. In GA, binary coding of the variables is often employed for convenience. Fitness is computed for every population before selection of the mating pairs. For selection of mating variables, either roulette wheel method or tournament selection can be used. Single-point crossover is commonly employed. Essentially,

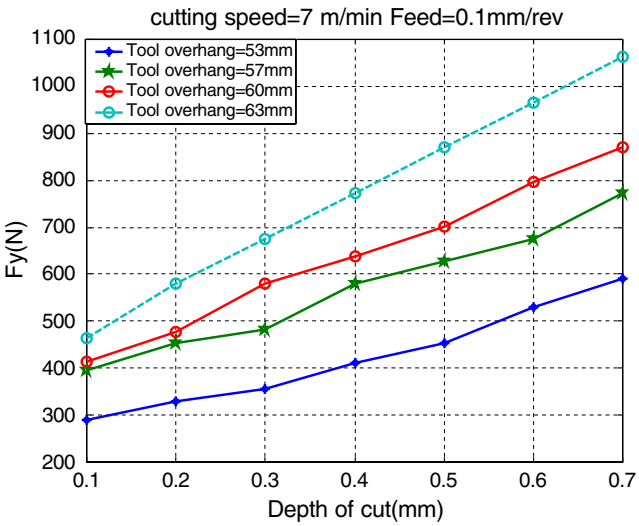

Fig. 4 Variation of radial force with DOC

GA is developed for unconstrained single objective optimization problems. Further details of GA can be found elsewhere [19]. In the present context, GA is used to obtain the optimal cutting variables which minimize all the three cutting forces. The formulation is written as:

$$\text{Minimize } f_{\text{op}}(v, f, d, l) = F_x + F_y + F_z \quad \text{Subjected to}$$
$$7 \le v \le 22,$$
$$0.1 \le f \le 0.5,$$
$$0.1 \le d \le 0.4,$$
$$53 \le l \le 63.$$

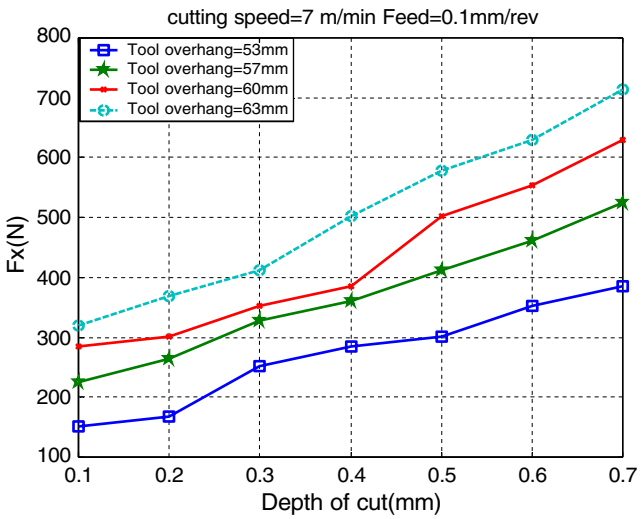

Fig. 3 Variation of feed force with DOC

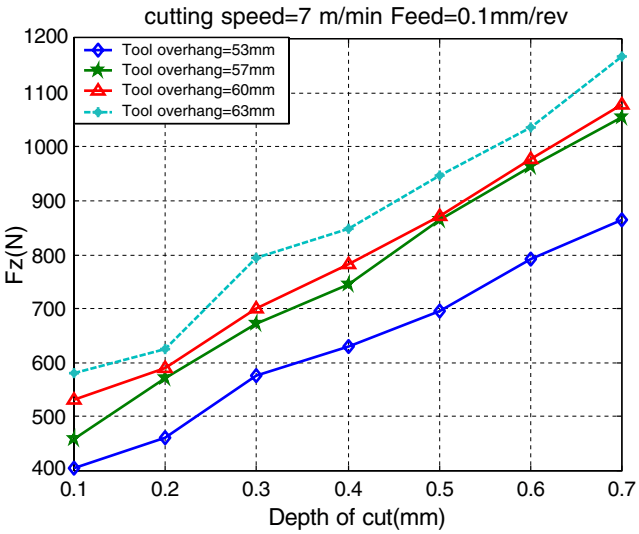

Fig. 5 Variation of tangential force with DOC

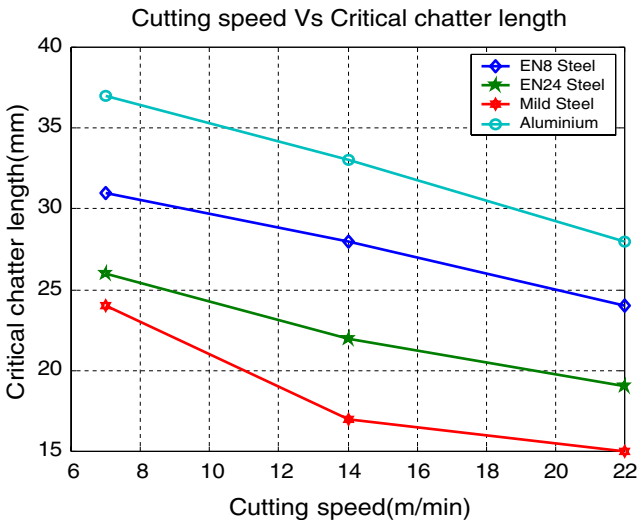

Fig. 6 Cutting speed (m/min)–CCL (mm)

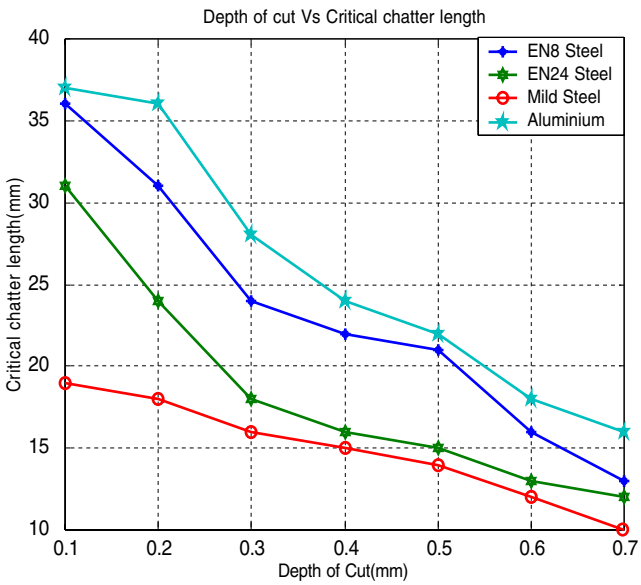

Fig. 8 DOC (mm)–CCL (mm)

4 Results and discussions

4.1 Effect of cutting parameters on cutting forces and critical chatter length

The critical chatter length is the distance between the point where the maximum force attained with violent sound and free end of the workpiece and this is related to process stability. The critical chatter length is recognized by the sudden increase in force which is indicated by the strain gauge dynamometer and these cutting forces shown in tables are the maximum values. Figures 3, 4, and 5 depict the variation of cutting forces as a function of depth of cut and tool overhang for EN8 steel workpiece operated at 7 m/min. It can be seen that the cutting forces increases, while the critical chatter length decreases with the depth of cut and tool overhang. However, the changes are not linear or uniform. Thus, output parameters are influenced simultaneously by the operating variables as well as tool overhang in nonlinear fashion. The effect of cutting speed, feed rate, and depth of cut on critical chatter length values for four workpiece materials is shown in Figs. 6, 7, and 8, respectively. From the Fig. 6, it is observed that at low-cutting speed, critical chatter length is high and vice versa. But from these results, it is observed that chatter depends on the material properties also. From the Fig. 7, it is observed that the critical chatter length decreases when the feed rate was increased. This was attributed to the fact that

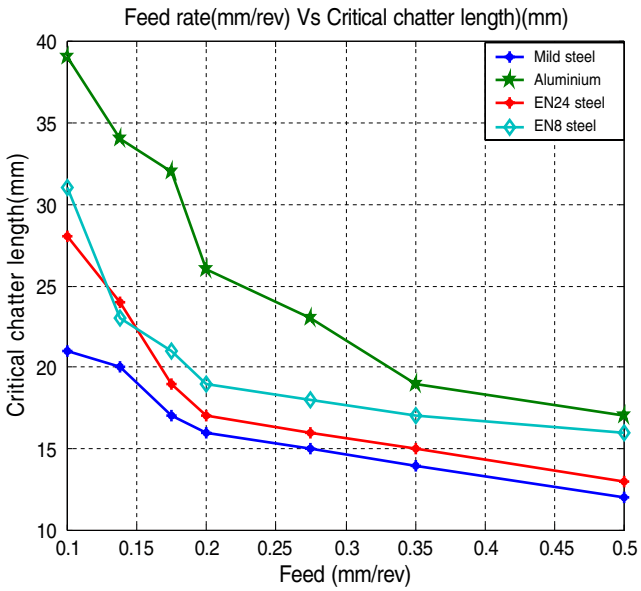

Fig. 7 Feed rate (mm/rev)–CCL (mm)

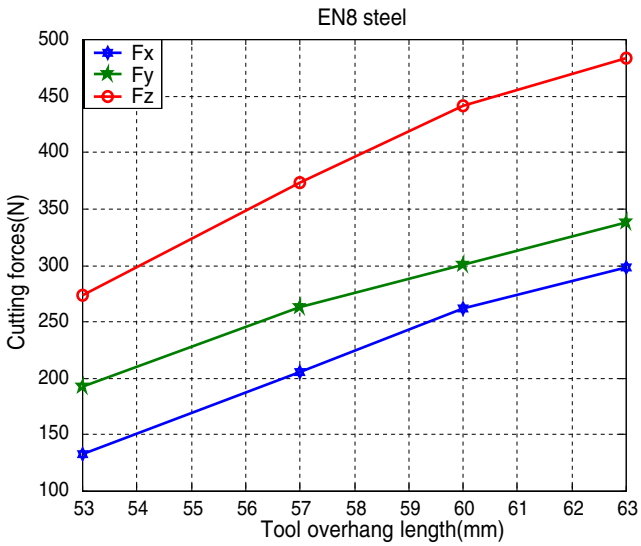

Fig. 9 TOL (mm)–cutting forces (N) for EN8 steel

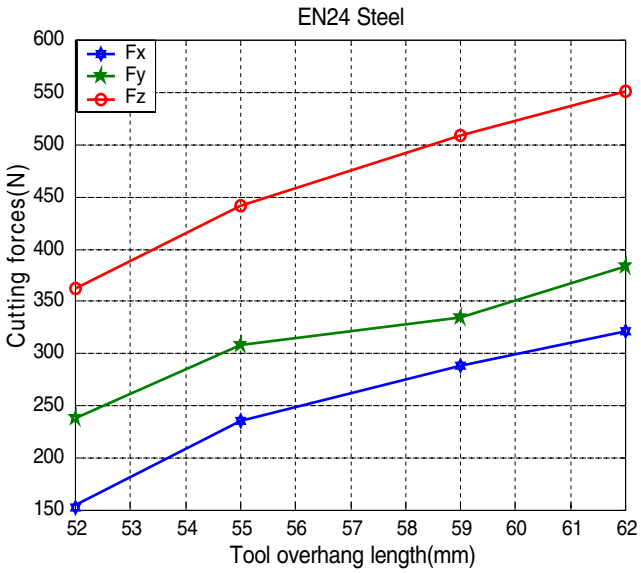

Fig. 10 TOL (mm)–cutting forces (N) for EN24 steel

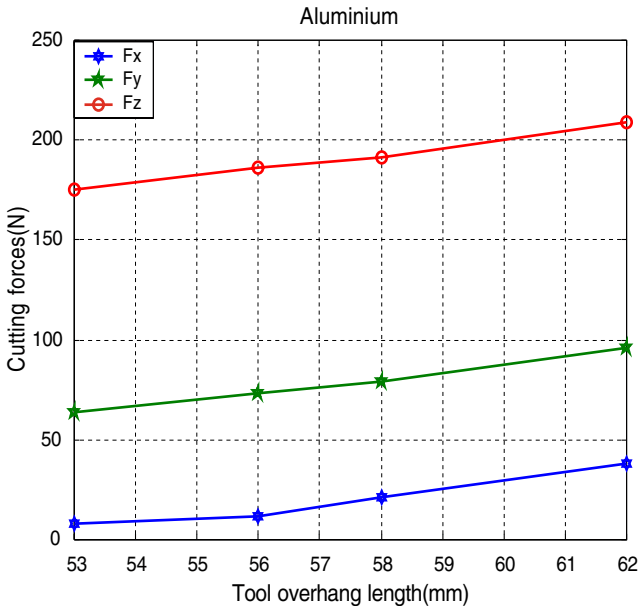

Fig. 12 TOL (mm)–cutting forces(N) for aluminum

the area of cut substantially increased per cycle of cut; hence, more shearing had to be done which required more force and there by decreases the critical chatter length. From the Fig. 8, it is observed that increasing the depth of cut generally resulted in a proportional decrease in critical chatter length.

4.2 Effect of tool overhanging length

Tool overhang is defined as the length by the tool extends from the tool holder. The length by which the tool extends from the tool holder is a variable that can be used to tune the machining process. When chatter occurs, the natural reflex is to reduce spindle speed, but increasing the speed may in fact be a more productive response. Another common response to chatter is to switch to a tool, because of the seeming stiffness of a shorter tool. Recent and ongoing experiments in the tool tuning of overhanging length have had encouraging results. Figure 9 shows the variation of cutting forces against the different tool overhanging lengths for EN8 steel and it is observed that radial cutting force sharply increases when tool overhanging length exceeds 59 mm. From the previous literature, it is known that large amount of positive radial force is undesirable. A large positive radial force causes the workpiece to deflect and there by surface finish deterio-

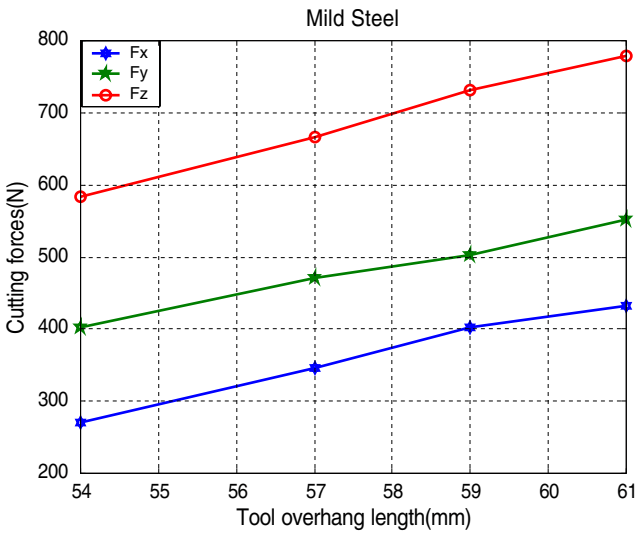

Fig. 11 TOL (mm)–cutting forces (N) for mild steel

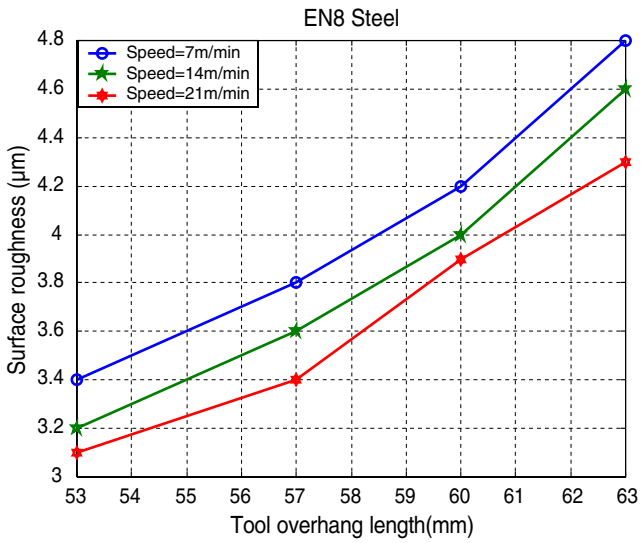

Fig. 13 TOL (mm)–surface roughness (μm) for EN8 steel

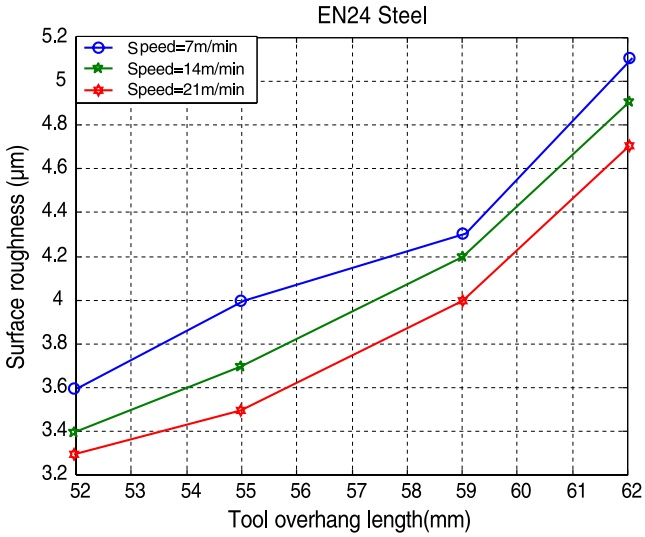

Fig. 14 TOL (mm)–surface roughness (µm) for EN24 steel

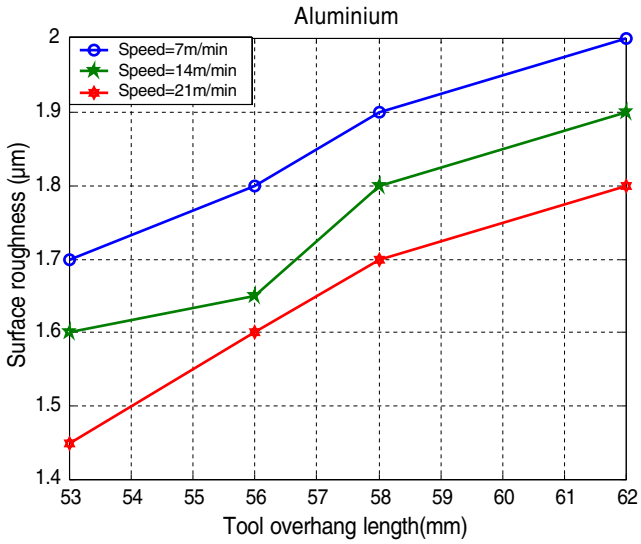

Fig. 16 TOL (mm)–surface roughness (µm) for aluminum

rates. Similarly, the influence of tool overhanging length on cutting forces is shown in Figs. 10, 11, and 12 for EN24 steel, mild steel, and aluminum, respectively. From the above three figures, it is observed that the cutting force is increasing along *X*, *Y*, and *Z* directions with an increase in tool overhanging length.

As tool overhanging is increased, the maximum roughness height increases which means the quality of surface deteriorates as shown in Fig. 13. Figures 14, 15, and 16 show the variation of surface roughness against the different tool overhanging lengths for EN24 steel, mild steel, and aluminum, respectively, at different cutting conditions and tool angles and thereby, critical chatter length decreases. On the other hand, critical chatter length decreases when the tool overhang length increases, i.e., instability increases as the tool overhanging length is increased as shown in Figs. 17, 18, 19, and 20 for EN8 steel, En24 steel, mild steel, and aluminum, respectively.

For each workpiece material, experimental results of 74 cases are selected as learning samples to train the neural network. The remaining ten sets are used as inputs to verify the accuracy of the model. Architecture has four input and five output nodes. Input–output data are first normalized in MS-Excel and the training and testing data are stored as text files. Four hidden nodes are selected based on several trails. The central vectors are obtained from K-means clustering algorithm. The learning parameter (α) is chosen as 0.4. Maximum number of cycles is selected as 500.

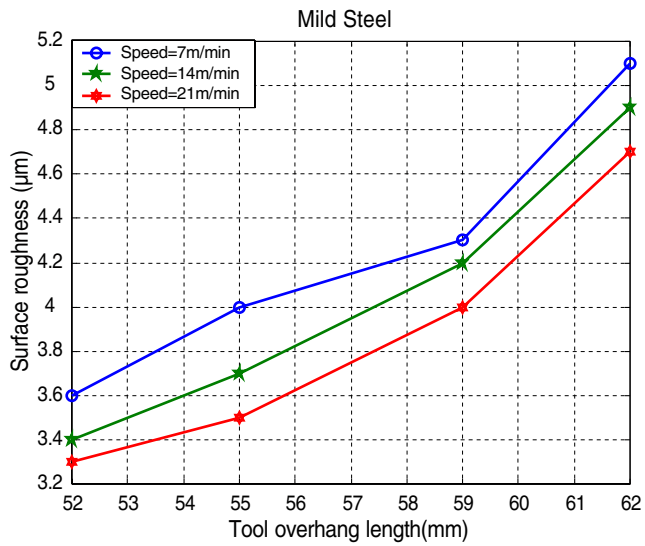

Fig. 15 TOL (mm)–surface roughness (µm) for mild steel

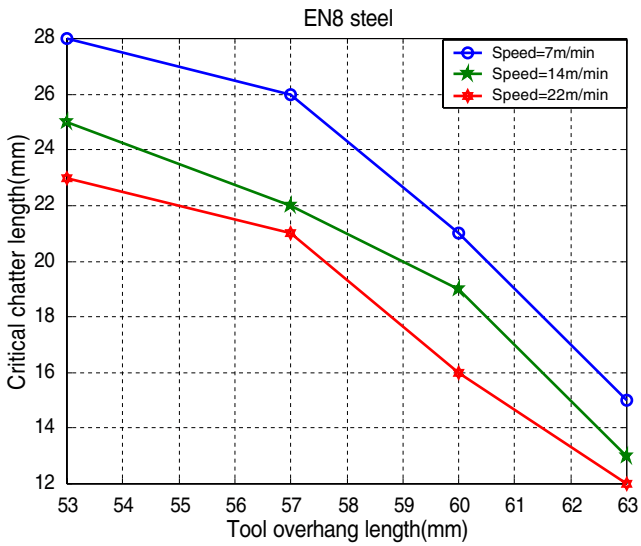

Fig. 17 TOL (mm)–CCL (mm) for EN8 steel

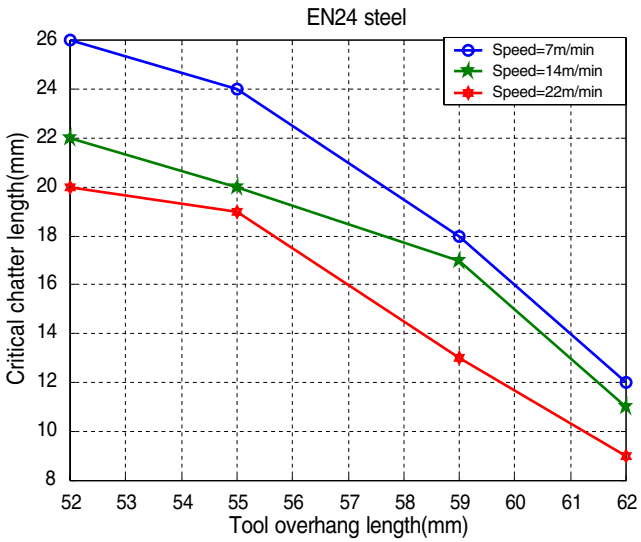

Fig. 18 TOL (mm)–CCL (mm) for EN24 steel

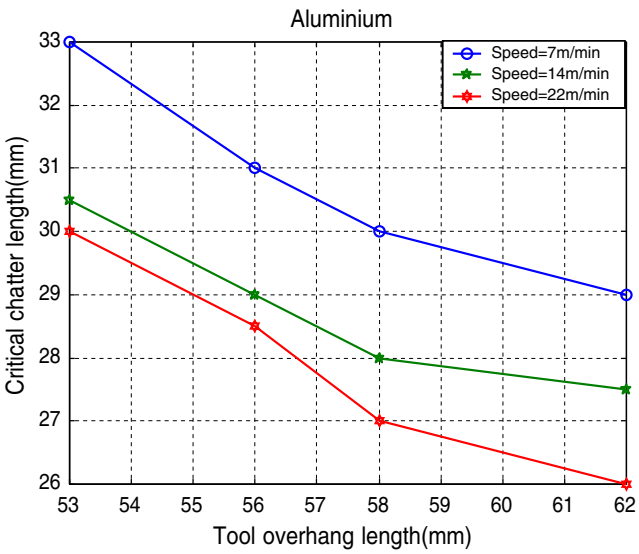

Fig. 20 TOL (mm)–CCL (mm) for aluminum

Figure 21 shows the progress of network training for σ_j=1. As σj is increased, the average predictions are found to be comparatively poor for EN8 steel. The network centers and weights are stored at this configuration.

The predicted outputs correspond to all the trained samples are very close to the target values. Table 2 shows the accuracy of predictions for all ten cases (data corresponding to results of experiments #75–84) of work materials EN8 steel, EN24 steel, mild steel, and aluminum. Even there is a noticeable deviation in few output variables, average accuracy of the model is found to be good. This may be due to the limited number of training cycles. After the neural network model is established correctly, the GA procedure is employed to determine the optimum cutting parameters. For obtaining the mating pairs, tournament selection approach is employed. In binary coding terminology, each population point is represented as a bit string made up of as many substrings as the number of variables. Here, each substring length is chosen as 10 (that is 10 b are used to represent each variable) and a population of 40 individuals is considered in each case. The crossover probability is considered as 98% and the probability of mutation is taken as 1%. The number of generations is selected as 200.The optimum machining parameters and corresponding maximum and minimum cutting forces as well as critical chatter lengths are obtained for each work material.

Table 3 shows some ranges of operating parameters and corresponding optimized forces F_x, F_y, F_z, and CCL, optimum cutting conditions v_o, d_o, and l_o predicted by GA

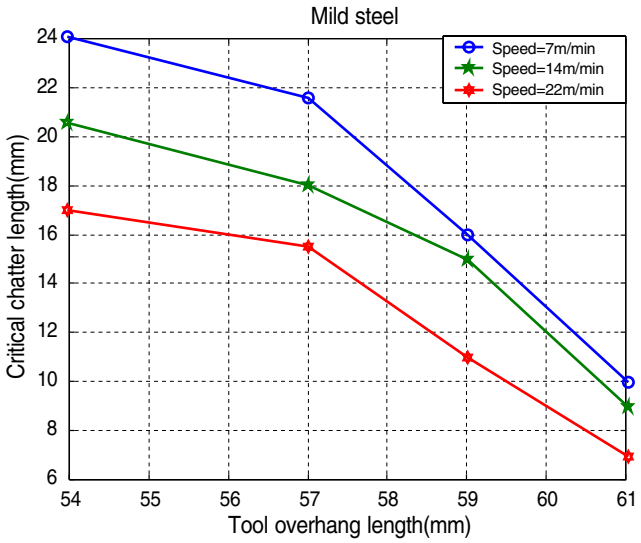

Fig. 19 TOL (mm)–CCL (mm) for mild steel

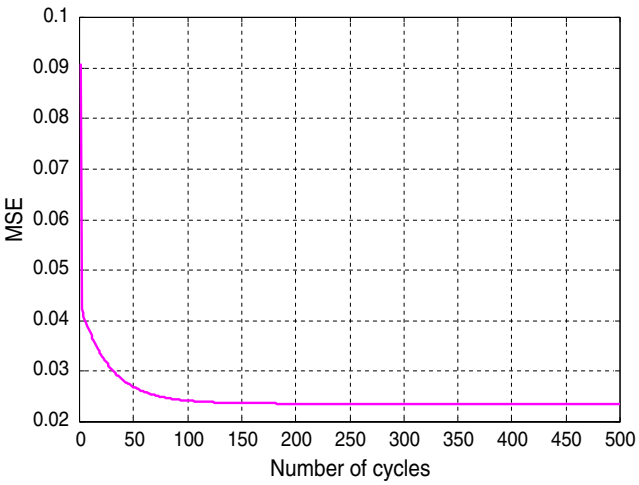

Fig. 21 Variation of mean square error during turning for EN8 steel

Table 2 Comparison of output values for EN8 steel and EN24 steel

SL. no	Material	F_x (N)		F_y (N)		F_z (N)		R_a (μm)		CCL (mm)	
		P	T	P	T	P	T	P	T	P	T
1	EN8 steel	463	484	616	606	764	781	3	3.1	13	12.5
2		524	531	645	641	824	819	3.6	3.6	10	10.4
3		596	585	733	735	858	848	3.9	4.1	8	8.6
4		351	354	410	417	586	576	0.9	1.1	24	22.5
5		404	403	504	505	644	659	1.5	1.3	18	17.4
6		446	451	613	608	690	707	2.8	2.9	15	14.6
7		463	460	677	666	754	746	3.1	3.0	11	11.4
8		514	509	704	713	830	835	3.5	3.7	9	8.5
9		562	568	710	721	890	905	4	4.1	8	7.6
10		648	655	808	810	958	971	4.3	3.9	6	7.9
11	EN24 steel	476	471	675	671	839	842	3.3	3.8	10	11.2
12		539	533	706	711	904	906	3.8	4.1	8	9.4
13		616	612	786	798	942	949	4	4.2	6	6.5
14		371	376	473	479	672	681	1.1	1.4	21	21.4
15		422	425	562	566	719	726	1.7	1.5	19	21.7
16		477	492	666	678	768	785	3.1	3.4	15	16.8
17		483	486	731	735	829	819	3.3	3.5	12	11.8
18		537	539	767	768	908	921	4	4.2	8	9.7
19		589	591	788	792	969	978	4.2	4.3	7	8.4
20		664	672	850	846	1,032	1,046	4.7	4.9	5	6.7
21	Mild steel	685	697	1,071	1,092	1,389	1,354	3.7	3.9	8	7.2
22		743	736	1,094	1,099	1,450	1,467	4.2	4.1	7	7.8
23		819	821	1,186	1,164	1,484	1,498	4.5	4.4	6	6.4
24		579	589	866	868	1,219	1,221	1.4	1.3	13	13.2
25		634	639	955	958	1,267	1,287	2.1	2.2	12	12.8
26		686	702	1,057	1,069	1,320	1,328	3.6	3.8	10	10.4
27		705	713	1,130	1,122	1,380	1,366	3.8	4.1	8	8.2
28		744	749	1,159	1,144	1,442	1,441	4.3	4.2	7	7.3
29		806	808	1,183	1,167	1,507	1,502	4.8	4.4	6	6.2
30		875	888	1,236	1,243	1,572	1,565	5.2	5.6	5	5.8
31	Aluminum	163	164	266	254	429	436	1.2	1.5	14	13.4
32		179	177	282	288	447	452	1.5	1.3	11	10.6
33		197	192	300	309	465	464	1.7	1.8	9	9.8
34		111	115	214	220	379	381	0.6	1.1	25	23.8
35		129	136	232	241	397	402	0.8	0.7	19	18.8
36		143	147	246	256	411	414	0.9	1.0	16	16.4
37		157	159	260	264	425	434	1.1	1.2	12	12.7
38		178	172	281	288	445	446	1.3	1.5	10	10.5
39		194	199	297	306	461	464	1.6	1.9	9	9.6
40		216	223	320	331	482	472	1.8	1.7	7	7.7

P predicted, *M* measured

program. As seen from tables, the optimum cutting parameters are the extremities of the selected cutting ranges. It is similar to earlier works in literature.

It is also observed that an increase in feed and depth of cut along with tool overhang rise the cutting forces, while the cutting forces in the experimental range has relatively less influence on the dynamics. Relatively high cutting forces are observed when mild steel workpiece is employed. The convergence time for each run to achieve the desired cycles is 8 s on X86 based PC with 3 GHz processor. The combined effect of all parameters could lead to better visualization at the shop floor level.

Table 3 Outputs of GA for different ranges of input variables

Material	V (m/min)	d (mm)	l (mm)	F_x (N)	F_y (N)	F_z (N)	SR (μm)	CCL (mm)	v_o (m/min)	d_o (mm)	l_o (mm)
EN8 steel	7–14	0.1–0.4	53–57	462.6	631.5	723.6	1.46	16.23	7	0.1	56.95
	7–14	0.1–0.4	57–63	466.8	631.0	723.8	1.35	16.21	7	0.1	63.00
	7–14	0.4–0.7	53–57	542.9	810.8	923.9	2.51	14.27	7	0.4	56.90
	7–14	0.4–0.7	57–63	539.3	808.6	923.3	2.45	14.28	7	0.4	62.97
	14–22	0.1–0.4	53–57	586.4	760.1	856.7	2.12	18.07	14	0.1	57.00
	14–22	0.1–0.4	57–63	591.5	755.4	857.2	2.14	18.12	14	0.1	57.00
	14–22	0.4–0.7	53–57	595.4	801.5	964.6	3.21	13.71	14	0.4	56.89
	14–22	0.4–0.7	57–63	601.5	785.0	966.5	3.23	13.12	14	0.4	62.95
EN24 steel	7–14	0.1–0.4	52–56	441.6	430.4	725.6	1.49	17.7	7	0.1	55.9
	7–14	0.1–0.4	56–62	489.8	513.8	912.5	1.38	14.8	7	0.1	61.9
	7–14	0.4–0.7	52–56	504.0	551.1	934.8	2.54	14.2	7	0.4	55.9
	7–14	0.4–0.7	56–62	584.0	631.8	921.3	2.49	13.0	7	0.4	62.0
	14–22	0.1–0.4	52–56	424.1	615.0	834.7	2.18	16.4	14	0.1	55.9
	14–22	0.1–0.4	56–62	430.3	623.3	788.6	2.19	16.2	14	0.1	61.2
	14–22	0.4–0.7	52–56	688.6	736.1	989.6	3.29	12.0	14	0.4	55.9
	14–22	0.4–0.7	56–62	689.9	737.8	998.7	3.28	12.2	14	0.4	61.5
Mild steel	7–14	0.1–0.3	54–57	598.6	888	1,334.2	1.86	9.64	7	0.1	56.9
	7–14	0.1–0.3	57–61	597.3	889	1,339.7	1.92	9.65	7	0.1	61.0
	7–14	0.3–0.5	54–57	620.2	1,032	1,443.2	2.96	7.73	7	0.3	56.9
	7–14	0.3–0.5	57–61	639.0	1,031	1,442.6	2.98	9.24	7	0.3	61.0
	14–22	0.1–0.3	54–57	773.9	1,175	1,556.8	3.85	8.96	14	0.1	56.9
	14–22	0.1–0.3	57–61	773.9	1,178	1,557.9	3.89	8.97	14	0.1	60.9
	14–22	0.3–0.5	54–57	716.7	1,224	1,587.3	4.67	8.57	14	0.3	56.8
	14–22	0.3–0.5	57–61	718.6	1,225	1,589.4	4.81	7.04	14	0.3	60.9
Aluminum	7–14	0.1–0.3	53–56	164.2	236.7	392.6	0.91	12.14	7	0.1	56.0
	7–14	0.1–0.3	56–62	164.4	236.8	392.8	0.94	12.06	7	0.1	61.5
	7–14	0.3–0.5	53–56	187.2	258.4	428.1	1.13	12.36	7	0.3	55.9
	7–14	0.3–0.5	56–62	188.1	258.9	428.6	1.14	12.32	7	0.3	61.8
	14–22	0.1–0.3	53–56	208.4	313.2	466.7	1.31	10.83	14	0.1	55.6
	14–22	0.1–0.3	56–62	208.7	313.4	466.7	1.31	10.54	14	0.1	61.9
	14–22	0.3–0.5	53–56	212.4	319.8	481.2	1.68	10.85	14	0.3	55.9
	14–22	0.3–0.5	56–62	212.6	319.9	481.2	1.69	10.89	14	0.3	61.9

5 Conclusions

In this paper, a multivariate model of orthogonal turning operation has been formulated based on series of experiments. Using the experimental data for different workpiece materials, the cutting dynamics is modeled with radial basis function neural network. Through neural network model of function, optimum operating variables namely speed, feed, depth of cut, and tool overhang lengths are established by minimizing total cutting force using GA. The corresponding chatter lengths are also reported. It is found that compared to speed, feed, depth of cut, and overhang of tool have profound influence on the cutting forces and critical chatter locations. Convergence would have been better when the neural network training is based on error criterion. The cutting forces are considerably affected by the variation of any one of the cutting variables. It is observed in the present investigation that the characteristics of the cutting force fluctuations in turning vary primarily with feed rate. The variation in the cutting speed seems to have very little influence on the cutting force components. In turning operations, feed rate is the most influential parameter on surface roughness, cutting depth is the second most one, and cutting speed is the least influential parameter. The influence of cutting speed is negligible compared with those of the other cutting parameters. At low cutting speed, critical chatter length from the free end of the workpiece is high that is by increasing the speed chatter comes earlier. But from this, results observed that chatter depends on the feed rate, depth of cut, and material properties also. The work can

be extended by considering the feed and depth of cut as simultaneous variables to obtain more practical model.

References

1. Rao BC, Shin YC (1999) A comprehensive dynamic cutting force model for chatter prediction in turning. Int J Mach Tools Manuf 39:1631–1654
2. Chiou RY, Liang SY (1998) Chatter stability of a slender cutting tool in turning with tool wear effect. Int J Mach Tools Manuf 38:315–327
3. Chandiramani NK, Pothala T (2006) Dynamics of 2-DOF regenerative chatter during turning. J Sound Vib 290:448–464
4. Chen CK, Tsao TS (2006) A stability analysis of turning a tailstock supported flexible work-piece. Int J Mach Tools Manuf 46:18–25
5. Berardos PG, Mosialos S, Vosniakos GC (2006) Prediction of workpiece elastic deflections under cutting forces in turning. Robot Comput Integr Manuf 22:505–514
6. Martínez JC, Ruiz CJ, Guzman AL (2008) Analysis of compliance between the cutting tool and the workpiece on the stability of a turning process. Int J Mach Tools Manuf 48:1054–1062
7. Azouzi R, Guillot M (1997) Online prediction of surface finish and dimensional deviation in turning using neural network-based sensor fusion International. J Mach Tools Manuf 37:1201–1217
8. Risbood KA, Dixit US, Sahasrabudhe AD (2003) Prediction of surface finish and dimensional deviation by measuring cutting forces and vibrations in turning process. J Mater Process Technol 132:203–214
9. Tangjitsitcharoen S, Moriwaki T (2007) Intelligent identification of turning process based on pattern recognition of cutting states. J Mater Process Technol 192:491–496
10. Dhar NR, Kamruzzaman AM (2006) Effect of minimum quantity lubrication (MQL) on tool wear and surface roughness in turning AISI-4340 steel. J Mater Process Technol 172:299–304
11. Gaitonde VN, Karnik SR, Davim JP (2008) Selection of optimum MQL and cutting conditions for enhancing machinability in turning of brass. J Mater Process Technol 204:459–464
12. Sekar M, Srinivas J, Rama Kotaiah K, Yang SH (2008) Stability analysis of turning process with tailstock-supported workpiece. Int J Adv Manuf Technol. doi:10.1007/s00170-008-1764-2
13. Jiao Y, Lei S, Pei ZJ, Lee ES (2006) Fuzzy adaptive networks in machining process modeling: surface roughness prediction in turning operations. Int J Mach Tools Manuf 44:1643–1651
14. Abburi NR, Dixit US (2006) A knowledge-based system for the prediction of surface roughness in turning process. Robot Comput Integr Manuf 22:363–372
15. Dhokia VR, Kumar S, Vichare P, newman ST, Allen RD (2008) Surface roughness prediction model for CNC machining of polypropylene. Proc Inst Mech E Part B J Eng Manuf 222:137–157
16. Lu C (2008) Study on prediction of surface quality in machining process. J Mater Process Technol 205:439–450
17. Cardi AA, Firpi HA, Bement MT, Liang SY (2008) Workpiece dynamic analysis and prediction during chatter of turning process. Mech Syst Signal Process 2:1481–1494
18. Haykin S (2001) Neural networks, a comprehensive foundation. Tsinghua University Press, Beijing
19. Goldberg D (1989) Genetic algorithms in search-optimization and machine learning. Addison-Wesley, Readings